Genomic analyses capture the human-induced demographic collapse and recovery in a wide-ranging cervid

Camille Kessler[1], Aaron B.A. Shafer[1,2]

[1]Environmental and Life Sciences Graduate Program, Trent University, 7K9J 7B8 Peterborough, Ontario, Canada

[2]Department of Forensic Science, Trent University, 2140 East Bank Drive, Peterborough, ON K9J 7B8, Canada

Correspondence: camillekessler@trentu.ca (CK), aaronshafer@trentu.ca (ABAS)

Abstract

The glacial cycles of the Quaternary heavily impacted species through successions of population contractions and expansions. Similarly, population demography has been intensely shaped by human pressures such as unregulated hunting and land use changes. White-tailed and mule deer survived in different refugia through the Last Glacial Maximum, and their populations were severely reduced after the European colonisation. Here, we analysed 73 re-sequenced deer genomes form across their North American range to understand the consequences of climatic and anthropogenic pressures on deer demographic and adaptive history. We found a strong signal of glacial-induced vicariance and demographic decline; notably, there is a severe decline in white-tailed deer effective population size (N_e) at the end of the Last Glacial Maximum. We found robust evidence for a colonial impact in the form of a recent and dramatic drop in N_e in all analysed populations. Historical census size and restocking data show a clear parallel to historical N_e estimates, but temporal N_e/N_c ratio shows patterns of conservation concern for mule deer. Signatures of selection highlight genes related to temperature, including a cold receptor previously highlighted in woolly mammoth. We also detected numerous immune-genes that we surmise reflect the changing land-use patterns in North America. Our study provides a detailed picture of anthropogenic and climatic-induced decline in deer diversity, and clues to understanding the conservation concerns of mule deer and the successful demographic recovery of white-tailed deer.

Keywords: Odocoileus, LGM, island population, human impact

Introduction

The glacial cycles of the Quaternary with ice sheet movement, corresponding sea level fluctuations, and global environmental changes, heavily impacted worldwide biota (Batchelor et al. 2019; Allen et al. 2020; Gowan et al. 2021). In the northern hemisphere, species adapted to temperate climate were forced to adapt in cold periods, move or retreat to refugia, their population decreasing or going extinct in the process, while warming episodes allowed for population expansion, colonisations, and adaptive divergence (Pamilo and Savolainen 2004; Lorenzen et al. 2011; Martchenko and Shafer 2023). The peopling of North America ~15,000 years ago (ka; Willerslev and Meltzer 2021) followed by human expansion was also a driver of regional ecological shifts (Gajewski et al. 2019; Fulton and Yansa 2021; Commerford et al. 2022), although there is no scientific consensus on whether they were responsible for large mammal declines (Stuart 2015; Meltzer 2020; Stewart et al. 2021).

The more recent Anthropocene has dramatically shaped demographic trajectories of wildlife through farming, hunting and logging (Ceballos et al. 2015; IPCC 2022). Human pressures substantially increased during colonial eras when settlers profoundly altered the land, leading to declines in endemic populations (Woinarski et al. 2015; Lindo et al. 2016; Tavares et al. 2019; Brain and Prosser 2022; Stevens et al. 2022). Indeed, colonial impact has been associated with the extinction of several species such as Australian rodents, or the blue antelope (*Hippotragus leucophaeus;* (Roycroft et al. 2021; Hempel et al. 2022). Beyond the demographic impacts, settler populations might also have altered selection pressures, recent examples of selective harvest include brown bears (*Ursus arctos*) or moose (*Alces alces*; Allendorf and Hard 2009; Kvalnes et al. 2016; Van De Walle et al. 2018).

Severe population contractions, or bottlenecks, increase genetic drift and inbreeding risk, and while highly deleterious mutations can be purged, mildly deleterious mutations tend to accumulate (Frankham 2005; Charlesworth 2009), as seen in alpine ibex (*Capra ibex*) and

55 woolly mammoth (*Mammuthus primigenius*; Palkopoulou et al. 2015; Grossen et al. 2020).
56 Population size fluctuations leave discernible genomic patterns: a declining population will
57 exhibit a positive Tajima's D and a relatively flat site frequency spectrum (SFS), whereas an
58 expanding population will present a negative Tajima's D and a SFS skewed towards low-
59 frequency alleles (Hahn 2018). Depending on the extent of the contraction, both in magnitude
60 and duration, populations might also present a low effective population size (N_e), particularly
61 if the bottleneck was strong and the recovery long (Martchenko and Shafer 2023). In contrast,
62 a population that remained steady over time, or one that recovered quickly from a bottleneck,
63 will usually exhibit a larger N_e (Charlesworth 2009). Genomic data can be used to model
64 changes in historical and, thanks to recent analytical advances, contemporary trends of N_e (Li
65 and Durbin 2011; Schiffels and Durbin 2014; Santiago et al. 2020; Schiffels and Wang 2020),
66 and when compared to census size (N_c), those estimates of N_e reflect adaptive potential and
67 extinction risk (Palstra and Ruzzante 2008; Wilder et al. 2023).

68 The species of the North American genus *Odocoileus* (deer) were heavily impacted by
69 the glacial cycles of the Pleistocene and European colonisation. Divergence estimates suggest
70 the speciation between white-tailed (*O. virginianus*; WTD) and mule deer (*O. hemionus*; MD)
71 took place between one and 3 million years (Ma; Wright et al. 2022; Kessler et al. 2023), the
72 genus became among the most successful Cervids during glacial cycles (Hewitt 2011). Both
73 species survived in different refugia during the Last Glacial Maximum (LGM, 26 - 19 ka (Clark
74 et al. 2009); Ellsworth et al. 1994; Greenslade 1998; Latch et al. 2009; Latch et al. 2014), and
75 while WTD & MD hybridise (eg. Carr and Hughes 1993; Russell et al. 2021), the hybridisation
76 appears to be a result of secondary contact and did not impact speciation (Kessler et al. 2023).

77 Deer abundance is heavily monetised through hunting-related activities (Cambronne
78 2013), and both species have been, and continue to be, important to indigenous communities
79 as a source of food, clothing and culture (Adams and Hamilton 2011; Peres and Altman 2018).

In the late Holocene, WTD were likely the most abundant large-mammal prey in eastern North America, and while some Indigenous People depended on them for subsistence, harvest appeared to minimally impact WTD numbers (Wolverton et al. 2008; Weitzel 2021). In contrast, over-hunting and forestry practices post-colonisation resulted in heavily depleted and even extirpated WTD populations, leading to strict hunting regulations and massive restocking efforts across the USA in the 20th century (McDonald et al. 2004), with stocking efforts leaving discernible patterns in WTD genome (Chafin et al. 2021; Wootton et al. 2023). Mule deer abundance is, and was, lower than WTD, but their populations also declined post-colonisation and plunged early 1900's (Jensen et al. 2023). Stocking efforts were much less pervasive for MD, and the species stabilised due to effective management strategies (Gruell 1986; Clements and Young 1997; Gill 1999; Bergman et al. 2015; Jensen et al. 2023). Previous historical demographic analysis for both species have generated both contrasting and coarse demographic scenarios (Combe et al. 2021; Lamb et al. 2021).

Here, we aim to understand the consequences of climatic and anthropogenic pressures on WTD & MD populations through explicit demographic modelling and selection analyses. We hypothesise that the population genetic histories of North American deer were heavily impacted by the glacial cycles of the Pleistocene and by European colonisation, not the initial peopling of North America. Specifically, we predict that the LGM had a strong negative impact in the form of demographic contraction and population subdivision, and that the impact of European colonisation, notably overhunting and change in land use, would leave detectable signatures on the genome in neutral and adaptive context. To test these predictions, we used WGS data of 73 deer to compute summary statistics, reconstruct and model demographic histories, and quantify genomic variation linked to environmental factors and selective forces.

Materials and Methods

Sampling & Sequencing

We sequenced the genomes of 45 deer collected across North America (Fig. 1A, Table S1) and added WGS data from 28 published deer genomes (PRJNA830519; Kessler et al., 2023). We extracted DNA using the Qiagen DNeasy Blood and Tissue Kit following manufacturer's instructions and checked concentration using Invitrogen Qubit assays. DNA was sent to The Centre for Applied Genomics in Toronto, Canada, for library preparation and sequencing. All samples were sequenced to an average of 4x coverage on an Illumina HiSeqX, except for four samples which were re-sequenced to achieve higher coverage (> 15x; Table S1, Fig. 1A). This 4x coverage was targeted as we generated genotype likelihoods that are designed for lower coverage data (Meisner and Albrechtsen 2018).

We obtained estimated census data for WTD and MD in the USA for the last 400 years from Webb (2018; complemented by Deer Friendly). This census data was generated using a process of environmental scanning that aggregated data from different sources such as state agencies, harvest records and historical sources for the most ancient timepoints. We also digitised restocking information for WTD in the USA from McDonald et al. (2004).

Data processing

We analysed and trimmed raw reads with FastQC (v0.11.9; Andrews 2010) and Trimmomatic (v0.36; Bolger et al. 2014), respectively. Using bwa-mem and default settings (v0.7.17; Li and Durbin 2009), we aligned raw reads to the WTD genome (GCA_014726795.1) and sorted the reads using SAMtools sort (v1.10; Li et al. 2009). We identified and removed duplicates in Picard MarkDuplicates (v2.23.2; Broad Institute, GitHub Repository. 2019) and Sambamba view (v0.7.0; Tarasov et al. 2015). We used GATK RealignerTargetCreator and IndelRealigner (v4.1.7.0; McKenna et al. 2010) to carry out a local re-alignment and used

129 Sambamba flagstat, mosdepth (v0.3.1; Pedersen and Quinlan 2018) and MultiQC (v1.10;
130 Ewels et al. 2016) for quality checks.

131 For samples sequenced on multiple lanes, we specified the read groups before removing
132 duplicates and merged the sequencing files using Picard AddOrReplaceReadGroups and
133 MergeSamFiles, respectively. To have a consistent coverage among samples for non-SMC
134 demographic analyses, we down-sampled data to the average coverage of all other samples
135 (4x) using Picard DownsampleSam. We called the genotypes (-doGeno 4) and estimated
136 genotype likelihood using the GATK model (-gl 2) in ANGSD (v0.918; Korneliussen et al.
137 2014). We retained SNPs with a minimum base quality and a minimum mapQ quality of 20 (-
138 minQ 20 & minMapQ 20) and a minimum p-value of 1e-6 (-SNP_pval 1e-6).

139 **Population subdivisions and summary statistics**

140 We used PCAngsd (v1.02; Meisner and Albrechtsen 2018) to investigate population
141 clustering between and within species, this program fits best our data as it is designed explicitly
142 for low-coverage data and genotype likelihoods. We investigated the relationship between the
143 spread on the PCA and the geographic distribution of our samples using a Pearson's correlation
144 test in R (v4.2.0; R Core Team 2021). To help decipher population structure in the MD samples,
145 we further ran NGSadmix (Skotte et al. 2013), using K = 1 : 10 and 10 replicates, we identified
146 the best K value using CLUMPAK (Evanno et al. 2005; Kopelman et al. 2015). We introduce
147 the following convention to refer to populations supported by PCAngsd and NGSadmix and
148 used in subsequent analyses: mainland WTD = WTD_{ML}, Florida Keys WTD = WTD_{KEY}, MD
149 subspecies = MD_{MD}, and MD black-tailed deer subspecies = MD_{BTD}.

150 We converted the hardcalls generated in ANGSD (.geno file) into a .vcf file using a
151 python script (genoToVCF.py; Martin 2021) and retained only biallelic sites (--max-alleles 2)
152 in VCFtools (v0.1.16; Danecek et al. 2011). Using VCFtools we computed weighted F_{st}
153 between the four populations, and Tajima's D and nucleotide diversity (π) per populations, all

154 three processed in windows of 50kbp. We used PLINK (v1.90b6.21; Chang et al. 2015) to
155 compute F_{ROH} on the 160 scaffolds representing the N90 of the WTD's genome assembly,
156 using the following non-default criteria: 100kb window size containing a minimum of 50 SNPs,
157 allowing up to three heterozygote sites and 10 missing calls per called ROH. We computed
158 F_{ROH} per individual using the sum of ROH sizes divided by the sum of N90 scaffolds length.

159 **Historical and recent demographic inference**

160 We inferred the historical demography of WTD_{KEY}, WTD_{ML}, MD_{MD} and MD_{BTD} by
161 implementing the multiple sequentially Markovian coalescent (MSMC) model (Schiffels and
162 Durbin 2014) that generates estimates of N_e over time. Here, we used four high-coverage
163 samples, one per population (Fig. 1A, Table S1), and first generated a 35-mer mappability
164 mask file using SNPable, as required for MSMC with several samples (Schiffels and Wang
165 2020). We phased the data with whathap (v1.3; Martin et al. 2016) and filtered out scaffolds
166 shorter than 500 Kbp. We ran MSMC2, including 100 bootstraps, using $1\times2+25\times1+1\times2+1\times3$
167 as time segment pattern. To estimate the cross-coalescence rate (CCR) across populations, we
168 carried out a pairwise comparison of the first haplotype from each sample using the -P flag,
169 skipping any site with ambiguous phasing. Finally, to test and account for ancestral migration,
170 we implemented MSMC-IM (Wang et al. 2020), assuming a generation time of 2 years
171 (Deyoung et al. 2003) and a mutation rate of $1.33\text{x}10^{-8}$ mutations/site/generation.

172 We used GONE (Santiago et al. 2020) to compute demographic history in the recent
173 past from patterns of linkage disequilibrium (LD) for the four populations. We restricted this
174 analysis to the 160 scaffolds representing the N90 of the WTD assembly. We ran GONE with
175 500 repetitions on 500 generations with 30,000 SNPs per chromosome, a minor allele
176 frequency pruning of 0.01, a hc value of 0.04, a recombination rate of 0.5 for WTD populations
177 and 0.35 for the MD populations (Kessler et al. 2023). We compared the census size (N_c) point

178 estimates from Webb (2018) to the temporal estimates of N_e resulting from GONE to obtain a
179 contemporary N_e/N_c ratio over time.

180 We further filtered the dataset in VCFtools to I) account for LD by removing sites that
181 were within 10kbp of each other (--thin 10000), and II) remove all missing data (--max-missing
182 1). To model explicitly the demographic history of WTD and MD, we used δaδi (v 2.1.1;
183 Gutenkunst et al. 2009) and dadi_pipeline (v3.1.7; Portik et al. 2017) and performed two
184 different demographic comparisons: 1) WTD_{KEY}, WTD_{ML} and all MD, and 2) MD_{MD}, MD_{BTD}
185 and WTD_{ML} as outgroup. We selected relevant models involving migration and asynchronous
186 splitting (Table S2), optimised and fitted the models with four repetitions and default settings,
187 the best model was selected based on the log-likelihood and its consistency across runs. This
188 model was additionally run with 100 bootstrapped frequency spectrums to quantify uncertainty.
189 We obtained ancestral N_e/N_c ratio over time for both species using the ancestral N_e (NuA) from
190 the δaδi analyses.

191 **Adaptive divergence and selection scans**

192 We used a redundancy analysis (RDA) to detect genotype-environment association and
193 loci under local adaptation across individuals. We first collected 19 bioclimatic variables
194 (Table S3) at a resolution of 2.5' from WorldClim2 using the R package raster (v.3.6-3;
195 Hijmans 2022; Fick and Hijmans 2017) and extracted the values corresponding to our samples'
196 coordinates. We performed three analyses: one inter-specific with all individuals, and two
197 intra-specific for WTD & MD using 19 bioclimatic variables, latitude, longitude, and species
198 as predictors. As highly correlated variables are problematic in RDAs, we removed those that
199 showed a Pearson correlation > 0.7 in each analysis (Dormann et al. 2013). We carried out the
200 RDA with the R package vegan (v.2.6-4; Oksanen et al. 2022) based on the datasets created
201 for demographic modelling. In addition to full models including non-correlated predictors, we

202 investigated conditional models with the condition set as either the bioclimatic variables or
203 longitude.

204 To detect regions under selection in the four populations, we computed the integrated
205 haplotype score (iHS) on the scaffolds representing the N90 of the WTD reference genome.
206 We started by phasing our data in SHAPEIT (v2.r904; O'Connell et al. 2014), then calculated
207 and normalised iHS in vcflib (v1.0.3; Garrison et al. 2022) with the functions iHS and
208 normalize-iHS and default settings. We identified peaks in the most extreme 1% iHS values in
209 R using the function findPeaks (Grinberg 2019) and extracted gene IDs within 25Kbp. The
210 genes with available entry IDs were uploaded to Uniprot (Pundir et al. 2016) for ID mapping
211 where we retrieved the gene names and functions. The gene list was manually curated, and
212 each gene was assigned to one or more of the following categories based on its function:
213 reproduction, immunity, physiology, metabolism, sensory perception, development, and other.
214 We analysed all results and produced all the graphics in R.

215 ## *Results*

216 **Population subdivisions and summary statistics**

217 We called 144,634,190 SNPs across species from 73 individuals at a coverage of 4x on
218 average. The PCA on allele frequencies of all individuals presents a clear species delimitation
219 along PC1 which explained 46% of the variation, whereas PC2 separated the WTD_{KEY}
220 individuals (Fig. 1B). WTD-specific PCA showed the delimitation between WTD_{ML} and
221 WTD_{KEY} individuals (PC1); PC2 strongly correlated with longitude (Pearson correlation = -
222 0.88, p-value = < 2.2e-16) and accounted for 7% of the variation (Fig. S1A). In the MD PCA,
223 PC1 correlated to longitude (Pearson correlation = 0.83, p-value = 5.96e-06), and PC2
224 associated to latitude (Pearson correlation = 0.47, p-value = 0.037, Fig. S1B). The MD PCA
225 showed one clear cluster of 13 samples; we clarified the population identity of the seven

226 remaining individuals using NGSadmix that assigned two admixed individuals to the first
227 cluster (MD_{MD}) and identified a second population of five individuals (MD_{BTD}; Fig. S1C).
228 Weighted F_{st} measures were very high in between species comparisons (0.36 - 0.58);
229 intra-specific comparisons ranged from 0.12 to 0.17 (Table S3). Tajima's D values were
230 positive only for the WTD_{KEY} population (0.11), the lowest being -0.89 for WTD_{ML} (Table 1).
231 F_{ROH} values were lowest in the MD populations (<= 0.3%), whereas WTD_{KEY} presented the
232 highest F_{ROH} value (1.4%; Table 1)

233 **Demographic inferences**

234 We inferred the demography of four high-coverage samples, one per population, using
235 MSMC2. The trajectories of the four samples split at approximately 600 ka where the MD_{MD}
236 population start declining whereas WTD populations keep increasing (Fig. 2A). Both MD
237 population trajectories are very similar and show a general steady decline. WTD_{KEY} appear to
238 decline ~50 ka, whereas WTD_{ML} drastically increased to peak at an N_e of >1 million
239 individuals, followed by a clear crash at the end of the LGM (Fig. 2A). Species split times
240 inferred by the cross-coalescence rate of the MSMC-IM model is approximately 500 ka (Fig.
241 S2A), the within-species split times are estimated at ~ 25 ka between WTD_{ML} and WTD_{KEY},
242 and ~70 ka for MD_{MD} and MD_{BTD} (Fig. S2B).
243 The N_e of WTD_{KEY} appears very low and stable for the last ~400 years, reaching its
244 lowest at ~350 individuals (Fig. 2B). Temporally, the WTD_{ML} population decreased with
245 variable intensity that ended with a drastic decline to a N_e of ~2000 near the end of the 19th
246 century. Following this severe drop, the WTD_{ML} population rapidly rebounded to reach a
247 current effective size in the millions (Fig. 2B); this clearly correlates with census data and
248 restocking efforts (Fig. 2C). Both MD populations exhibited a slow but steady increase until
249 approximately 300 years ago, after which both trajectories show a gradual decline ending with
250 a severe drop without recovery (Fig. 2B). MD N_e patterns are more decoupled from the census

251 data as N_c here shows a crash in both MD_{MD} and MD_{BTD} followed by a small recovery (Fig.
252 2C). As such, the contemporary N_e/N_c ratio is higher and more variable for MD (Fig. 3; mean
253 = 0.49, var = 0.3 vs WTD mean = 0.18 & var = 0.01) with most values from the last century
254 below 0.1. Both species have a low ancestral N_e/N_c ratio with low variability, the averages are
255 of 0.06 and 0.01 for WTD and MD, respectively. WTD's historical ratio (var = 0.03) is more
256 variable than MD's (var = 0.0001) and the contemporary WTD (Fig. 3).

257 Finally, we modelled the demographic history of our four populations using the site
258 frequency spectra. For our first comparison, we analysed the demographic history of the trio
259 WTD_{KEY} – WTD_{ML} – MD, the best model supports adjacent secondary contact between
260 populations, however migration rates remain low ($m < 1e^{-5}$; Fig. 4A, Table 2). This model
261 suggests a MD/WTD split ~260 ka followed by a MD decline and a WTD expansion. After the
262 split between WTD_{KEY} and WTD_{ML}, both populations declined with notably a demographic
263 crash in WTD_{KEY}; all of these predate the peopling of North America. In our second trio, we
264 investigated the relationship between MD_{MD} – MD_{BTD} – WTD_{ML}. In this case, the split
265 WTD/MD is seen ~230 ka, the best model suggests a secondary contact between WTD_{ML} –
266 MD_{MD} that predates the split between the two MD populations, ~12 ka, but all migration rates
267 are extremely low ($m < 1e^{-6}$). This model also suggests population expansion for WTD_{ML} but
268 a decline for both MD_{BTD} and MD_{MD} after the peopling of North America (Fig. 4B, Table 2).

269 **Adaptive divergence and selection**

270 We conducted three redundancy analyses to identify genotypes linked to environmental
271 variables and loci under local adaptation. The RDA with all individuals explained 16.5% of
272 the variation, most of which was driven by the species variable (Table 3, Fig. S5A). The full
273 model for the WTD explained 6.32% of the variation and included five significant predictors -
274 BIO1 (annual mean temperature), BIO2 (mean diurnal range), BIO8 (mean temperature of
275 wettest quarter), BIO15 (precipitation seasonality) and longitude (Table 3, Fig. S5B). There

276 were 12,206 outlier SNPs, predominantly associated with annual mean temperature (Table 3
277 & S3, Fig. S5C). In the RDA on MD, we found only BIO2 and BIO16 (precipitation of wettest
278 quarter) as significant predictors, and 7434 outlier SNPs, mostly associated with BIO16 (Table
279 3). Conditional models of bioclimatic variable explained more variation than those of longitude
280 in both species (Table 3).

281 We found a total of 443 genes within 25 Kbp of an iHS peaks, including 249 with an
282 existing Entry ID (Table S4). There were 121 genes around iHS peaks in the WTD_{ML}
283 population, 45 of which we could assign an explicit category including 18 genes assigned to
284 immunity, of which two related to the major histocompatibility complex (MHC): *HLA-DQA1*
285 and *HLA-DQB*. Additionally, we found two genes linked to sensory perception: one odorant
286 receptor (*OR5D18*) and one cold receptor (*TRPM8*, Table S4). We identified 23 genes
287 surrounding iHS peaks in the WTD_{KEY}, including one MHC gene: *HLA-DRB4*. For the MD_{MD}
288 population, we could explicitly categorise 34 genes on a total of 95 neighbouring iHS peaks.
289 They include four MHC genes: *HLA-DQA1*, *HLA-DQB1*, *HLA-DRB3* and *HLA-DRB4,* another
290 gene related to the MHC: *HIVEP2*, three genes described as olfactory or odorant receptors
291 (*OR51I1*, *OR5D18*, *TAAR5*), and one cold receptor (*GRIK2*). Finally, we identified 26 genes
292 adjacent to iHS peaks in the MD_{BTD} population, including two related to immunity and three
293 linked to reproduction.

Discussion

The complex climatic cycles of the Pleistocene, concluding with the LGM, generally forced species to move from a wide range into smaller, often isolated refugia (Shafer et al. 2010). The peopling of North America and the colonisation by Europeans several millennia later represented further pressures to many populations inhabiting the continent (McDonald et al. 2004; Lindo et al. 2016; Smith et al. 2021). Here, we reconstructed the demographic history and signals of selection of WTD & MD to improve our understanding of climatic and anthropogenic pressures on these two North American species. Through extensive genomic analysis we observed a remarkable overlap between climate, recent human drivers and N_e, and provide a temporal N_e/N_c assessment supporting the demographic concerns facing MD (Bergman et al. 2015; Webb 2018). Further, our selection scans that reflect climate and immunology pressures provide testable hypotheses for the impact of European colonisation.

Strong historical climatic impact on deer populations

The glacial cycles of the Quaternary forced populations to move or adapt, resulting in population divergence (Colella et al. 2021; Ito et al. 2021), decline (Ersmark et al. 2019; Baca 2020; Dussex et al. 2020; Meiri et al. 2020) and even replacement (Loog et al. 2020). Our results suggest a clear impact of climate on mainland WTD during the late Quaternary as we observed an intense N_e drop that coincides with the LGM for this population (Fig. 2A), and supports WTD populations being separated into different refugia during this period (Ellsworth et al. 1994; Moscarella et al. 2003; Combe et al. 2021; Wright et al. 2022). Similarly, the Key deer (*O. v. clavium*) showed a steady decline that predated the LGM, with a clear separation from WTD_{ML} ~50 ka (Fig. 2A, Table 2). While the CCR puts the population split time closer to the LGM (~20 ka; Fig. S2A), all analyses suggest both populations started diverging before the isolation of the Florida Keys from the continent ~8,000 years ago (Ellsworth et al. 1994; Villanova et al. 2017). This separation and isolation led to a clear loss of genomic diversity

319 and accumulation of deleterious alleles in the Florida keys (Table 1, Cars et al. 2023), and they
320 are currently listed as Endangered (U.S. Fish & Wildlife Service 1967). The collective
321 demographic methods here accurately pinpoint the LGM as a driver of subdivision and
322 historical declines in WTD.

323 The LGM has also been implicated in the MD_{MD} and MD_{BTD} division, as subspecies
324 were separated in different refugia during that time (Latch et al. 2009; Latch et al. 2014; Wright
325 et al. 2022). Our results are somewhat equivocal regarding the split time: the MSMC analysis
326 suggest a steady decline of both populations and the MD/BTD split estimated at approximately
327 70 ka (Fig. 2A, S2B); δaδi analysis, in slight contrasts, places the split during the LGM and
328 concomitant with a decline of ~70% in both populations (Table 2). Both analyses support
329 changes pre-peopling of North America and are consistent pre-split: the common ancestor of
330 MD_{MD} and MD_{BTD} appeared low, but stable through time, in stark contrast to the WTD
331 populations (Fig. 2A). As MD are more prone to population fluctuations (Forrester and
332 Wittmer 2013), and N_e is most strongly influenced by long periods of low N_c (Peart et al. 2020),
333 the overall stable historical N_e is consistent with population genetic theory.

334 Hahn (2018) suggested to focus on big picture and not point estimates for demographic
335 inferences. While the general historical patterns of demographic change observed here support
336 previous assessments (Lamb et al. 2021), including the LGM impact in WTD, they are in
337 contradiction with Combe et al. (2021). Combe et al. performed a stairway plot analysis of
338 ~25k SNPs; simulations have shown that a data set of this size is unlikely to reliably resolve
339 changes in N_e via site-frequency-spectra (Shafer et al. 2015), and thus our explicit modelling
340 and genome-wide data set has significantly more power and precision with respect to historical
341 demographic inference.

342 Hybridisation between WTD and MD in areas of sympatry is well documented (eg.
343 Cronin 1991; Derr 1991; Carr and Hughes 1993) but it was suggested that introgression had

344 no impact on the divergence of the species and rather that gene flow is a result of secondary
345 contact (Kessler et al. 2023). This is consistent with our analyses as both δaδi comparisons
346 suggest a secondary contact (Fig. 4), and while MSMC-IM and the δaδi analysis with WTD_{ML}
347 as outgroup still infers some ancient migration, it is extremely low (Table 2, Fig. S2C). Our
348 results therefore support the finding of negligible ancient gene flow between species.

349 **Human-induced collapse, varying selection pressures on white-tailed deer**

350 Driven by overharvest and change in land use for agriculture and logging, the recent
351 decline and near extirpation of WTD has been thoroughly documented in the USA (McDonald
352 et al. 2004). The reconstructed demographic trajectory of the mainland WTD population mirror
353 these historical sources and census size estimates (Fig. 2B-C); specifically, we capture the
354 gradual decline followed by dramatic collapse at the end of the 19th century. This depletion led
355 authorities to implement protective laws and managers to supplement deer populations with
356 translocations (McDonald et al. 2004). Those measures are responsible for the quick rebound
357 we observed for the WTD_{ML} population (Fig. 2B) as analyses of the nearly extirpated
358 populations of Mississippi and Missouri suggest the bottleneck of WTD populations had
359 minimal impacts on diversity thanks to the rapid population expansion following translocations
360 (Deyoung et al. 2003; Budd et al. 2018). Together with the stable relationship of N_e/N_c over
361 time we observed (Fig. 3), these results suggest that WTD is highly resilient. However, despite
362 the recovery and high diversity, a detailed assessment of deleterious alleles also showed a high
363 genetic load for WTD (Cars et al. 2023; Wootton et al. 2023), with a putative link to stocking
364 efforts (Wootton et al. 2023).

365 Given the low N_e and stocking efforts of WTD, it is probable that any sweep that took
366 place before the demographic collapse was either lost or fixed, with the latter generally having
367 reduced power in haplotype scans (Szpiech 2021). Further, and in contrast to ungulates
368 experiencing reduced human intervention (Martchenko and Shafer 2023), longitude had a

369 minimal impact in our models which is consistent with stocking efforts erasing historical
370 adaptive signals. Combined with evidence showing rapid contemporary evolutionary responses
371 (Zamorano et al. 2023), we suggest that the outliers and sweeps detected in our analyses could
372 be the result of selection post-European colonisation. In mainland WTD, we found a wide
373 variety of immunity-related genes, including two MHC genes potentially under selection which
374 would suggest selection pressures from pathogens (Table S4). WTD are subject to many
375 diseases, some of which have arisen recently from livestock, such as the epizootic
376 haemorrhagic and chronic wasting disease, as well as a variety of tick-borne diseases
377 (Campbell and VerCauteren 2011). While immune genes are often detected in genome scans,
378 their presence in WTD scans is consistent with the development of agriculture and large land
379 use changes that have transpired in North America over the past two centuries. This hypothesis
380 is testable through analysis of historical samples as any regions showing a sweep signal should
381 not exist in pre-colonial samples.

382 We also found selection patterns at the gene *TRPM8* conferring sensitivity to cold
383 temperature (Table S5); mutations identified in woolly mammoth's *TRPM8* were suggested to
384 be linked to the species' adaptation to cold climates (Lynch et al. 2015). Interestingly, in the
385 RDA between species, as well as in the WTD RDA, most outlier SNPs are associated with
386 mean annual temperature (BIO1) rather than species or longitude meaning that temperature is
387 a major driver of differentiation. WTD are exposed to a wide range of temperatures on the
388 continent, but also rapidly expanding northward (Dawe and Boutin 2016). As climate change
389 clearly impacted historical and contemporary WTD ranges (Dawe and Boutin 2016), outliers
390 and selection on genes like *TRPM8* are expected, and likely responsible for the success of WTD
391 on the continent.

392

393

Delayed collapse but similar selection pressures on mule deer

Human Settlements on the MD historic range were estimated at less than 20 in 1800, and while harvest likely depressed populations in the surrounding areas, the rest of the range probably saw minimal impact (Jensen et al. 2023). Over time and with the increased settlements in western North America, MD populations strongly declined to reach their lowest at the end of the 19th century (Gill 1999; Bergman et al. 2015; Jensen et al. 2023). This is consistent with our analysis which shows a sharp decrease in the MD_{MD} population during that period, though the MD_{BTD} population decline appeared later (Fig. 2B). These population reductions also appeared to happen after the WTD collapse, possibly reflecting the later western wave of settlers and more recent land use changes as a migrating species MD might respond more to human-induced habitat change. For example, the limitation in winter range habitat appears to be driving MD decline in Colorado (Gill 1999; Bergman et al. 2015). Thus, collectively the delayed and decoupling of N_e from N_c (Fig. 3), and more muted temporal response of N_e, is consistent the species ecology and human intervention history. Despite this collapse, both MD subspecies exhibit relatively high genetic diversity and low F_{ROH} (Table 1), all promising signals for a species that is often described as declining. Assessment of MD genetic load should help further inform the management challenges facing this species.

In MD_{MD}, we found many immunity-related genes under selection, including one MHC gene unique to this population (*HLA-DRB3*, Table S4). Diseases affecting MD are often the same that infect WTD, including the risk of spilling over to and from livestock (Campbell and VerCauteren 2011). Chronic wasting disease is of particular concern for MD: it is considered as a major factor in the species decline in many regions (DeVivo et al. 2017), with the genomic and immune response clearly polygenic (Seabury et al. 2020). Regarding sensory perception, we found selection patterns at the cold receptor *GRIK2*. Cold adaptation might have been a determinant factor for MD as they favour higher elevation habitats (Anthony and Smith 1977;

419 Brunjes et al. 2006), and are more tolerant to cold climates (Mautz et al. 1985). Supporting this
420 was outliers associated with mean diurnal range, which is linked to temperature (Table S4).
421 Most outlier SNPs were associated with precipitation of the wettest quarter (Table 3), likely
422 reflective of MD_{BTD} inhabitation of temperate rainforests (Heffelfinger and Krausman 2023).

423 **Variable N_e/N_c ratio through time**

424 The N_e/N_c ratio is informative on the genomic health and demographic histories of
425 species, which is why it has often been used to assess populations of management and
426 conservation concern (Frankham 1995; Palstra and Ruzzante 2008; Ferchaud et al. 2016).
427 Indeed, a population exhibiting a low contemporary N_e/N_c ratio is more subject to rapid loss in
428 genetic diversity than populations with a higher ratio (Frankham 1995; Palstra and Ruzzante
429 2008). While, this ratio is highly variable between taxa, the generally accepted median of
430 concern in wild populations is 0.1 (Frankham 1995; Waples et al. 2013). Our unique integrated
431 approach allowed use to measure this ratio over time, with the seven most recent values for
432 MD all below 0.1 (Fig. 3). The larger fluctuations in MD's N_c in the last 100 years appear to
433 have led to a decoupling of N_e and N_c and reflect the species higher demographic stochasticity.
434 This recent reduced ratio could mean that the species is at risk of faster loss of genetic diversity
435 and echoes other calls of concern (Gill 1999; Bergman et al. 2015). Interestingly, historical
436 N_e/N_c ratio presents low variability for both species and no immediate red flag (Wilder et al.
437 2023); this ratio is clearly driven by the high N_c of both species, and focused sampling of
438 isolated populations might reveal a different pattern as seen in caribou (Dedato et al. 2022).

439 ## *Conclusion*

440 We observed strong signals of climate- and human-induced demographic declines with
441 a remarkable overlap between both census and biogeographic data and historical inferences
442 coming from multiple methods. The dramatic drop in N_e in the recent past of all deer
443 populations studied here is robust evidence for a colonial impact through unregulated hunting

and changes in land use. Even though WTD & MD populations were heavily depleted, both species showed signs recovery, particularly white-tailed deer from restocking efforts. While diversity and demographic trends appear positive, there is also a high genetic load in WTD (Wootton et al. 2023), and a low contemporary N_e/N_c ratio in MD. Selection surrounding a wide variety of genes, including some of biological importance in WTD & MD such as genes related to immunity and temperature appear evident. Historical sampling of *Odocoileus* will prove informative for disentangling human-induced selection and genetic load in these wide-ranging cervids.

Acknowledgements

Camille Kessler was supported by an International Graduate Scholarship. This work was supported by NSERC Discovery Grant (Grant Number: RGPIN-2017- 03934); ComputeCanada Resources for Research Groups (Grant Number: RRG gme-665-ab); Canadian Foundation for Innovation: John R. Evans Leaders Fund and the Ontario Early Researcher Award (Grant Number: #36905). For providing samples, we thank Alan Cain, Steeve Côté, Anh Dao, Marco Festa-Bianchet, Brad Fulk, Eric Hoffman, Levi Jaster, Daniel Koelsch, Emily Latch, Brent Patterson, Joe Nocera, Don Stewart & Russell Easy, Jonathan Shaw, David Walter and Jon Wheeler. We also thank Jose Alberto López Alemán for commenting on the text.

We sampled deer from across North America, a stolen land which remains a home to many First Peoples and Trent University is located on the traditional territory of the Michi Saagiig Anishnaabeg. As settlers, we are grateful to have had the opportunity to live and work on this land, and to benefit from it. We would like to show our respect to the First Peoples and thank them for their care, stewardship, and teachings. Miigwetch.

Data Accessibility

Raw reads for the 45 deer additional individuals were deposited on the NCBI Sequence Read Archive (Accession number PRJNA830519). All scripts are available on GitLab (https://gitlab.com/WiDGeT_TrentU/graduate_theses/-/tree/master/Kessler/CH_02).

Author contributions

CK and ABAS conceived the study, ABAS collected the samples, CK performed the molecular laboratory work and the bioinformatic analyses with contribution from ABAS for MSMC2, CK and ABAS wrote the manuscript.

Declaration of interests

CK and ABAS declare no competing interests.

References

Adams KP, Hamilton RJ. 2011. Management History. In: Hewitt DG, editor. Biology and management of white-tailed deer. Boca Raton: CRC Press. Available from: http://site.ebrary.com/id/11007093

Allen JRM, Forrest M, Hickler T, Singarayer JS, Valdes PJ, Huntley B. 2020. Global vegetation patterns of the past 140,000 years. *J Biogeogr* 47:2073–2090.

Allendorf FW, Hard JJ. 2009. Human-induced evolution caused by unnatural selection through harvest of wild animals. *Proc. Natl. Acad. Sci. U.S.A.* 106:9987–9994.

Andrews. 2010. FastQC: a Quality Control Tool for High Throughput Sequence Data. Available online at: http://www.bioinformatics.babraham.ac.uk/projects/fastqc.

Anthony RG, Smith NS. 1977. Ecological Relationships between Mule Deer and White-Tailed Deer in Southeastern Arizona. *Ecological Monographs* 47:255–277.

Baca M. 2020. Diverse responses of common vole (Microtus arvalis) populations to Late Glacial and Early Holocene climate changes - Evidence from ancient DNA. *Quaternary Science Reviews*:13.

Batchelor CL, Margold M, Krapp M, Murton DK, Dalton AS, Gibbard PL, Stokes CR, Murton JB, Manica A. 2019. The configuration of Northern Hemisphere ice sheets through the Quaternary. *Nat Commun* 10:3713.

Bergman EJ, Doherty PF, White GC, Holland AA. 2015. Density dependence in mule deer: a review of evidence. *Wildlife Biology* 21:18–29.

Bolger AM, Lohse M, Usadel B. 2014. Trimmomatic: a flexible trimmer for Illumina sequence data. *Bioinformatics* 30:2114–2120.

Brain RA, Prosser RS. 2022. Human induced fish declines in North America, how do agricultural pesticides compare to other drivers? *Environ Sci Pollut Res* 29:66010–66040.

Broad Institute, GitHub Repository. 2019. "Picard Toolkit." Available from: http://broadinstitute.github.io/picard/

Brunjes KJ, Ballard WB, Humphrey MH, Harwell F, Mcintyre NE, Krausman PR, Wallace MC. 2006. Habitat Use by Sympatric Mule and White-Tailed Deer in Texas. *Journal of Wildlife Management* 70:1351–1359.

Budd K, Berkman LK, Anderson M, Koppelman J, Eggert LS. 2018. Genetic Structure and Recovery of White-tailed Deer in Missouri. *Jour. Wild. Mgmt.* 82:1598–1607.

Cambronne A. 2013. Deerland: America's Hunt for Ecological Balance and the Essence of Wildness. Available from: http://www.freading.com/ebooks/details/r:download/MDAwMDA5LTEwOTA1NDYz

Campbell TA, VerCauteren KC. 2011. Diseases and Parasites. In: Biology and management of white-tailed deer. Boca Raton: CRC Press. p. 220–240. Available from: http://site.ebrary.com/id/11007093

Carr SM, Hughes GA. 1993. Direction of Introgressive Hybridization between Species of North American Deer (Odocoileus) as Inferred from Mitochondrial-Cytochrome-b Sequences. *Journal of Mammalogy* 74:331–342.

Cars BS, Kessler C, Hoffman EA, Côté SD, Koelsch D, Shafer ABA. 2023. Island demographics and trait associations in white-tailed deer. Genomics Available from: http://biorxiv.org/lookup/doi/10.1101/2023.08.01.551454

Ceballos G, Ehrlich PR, Barnosky AD, García A, Pringle RM, Palmer TM. 2015. Accelerated modern human–induced species losses: Entering the sixth mass extinction. *Sci. Adv.* 1:e1400253.

Chafin TK, Zbinden ZD, Douglas MR, Martin BT, Middaugh CR, Gray MC, Ballard JR, Douglas ME. 2021. Spatial Population Genetics in Heavily Managed Species: Separating Patterns of Historical Translocation from Contemporary Gene Flow in White-tailed Deer. *Evol Appl* 14:1673–1689.

Chang CC, Chow CC, Tellier LC, Vattikuti S, Purcell SM, Lee JJ. 2015. Second-generation PLINK: rising to the challenge of larger and richer datasets. *GigaSci* 4:7.

Charlesworth B. 2009. Effective population size and patterns of molecular evolution and variation. *g e n e ti c s*:11.

Clark PU, Dyke AS, Shakun JD, Carlson AE, Clark J, Wohlfarth B, Mitrovica JX, Hostetler SW, McCabe AM. 2009. The Last Glacial Maximum. *Science* 325:710–714.

Clements D, Young A. 1997. A viewpoint: Rangeland health and mule deer habitat. *JOURNAL OF RANGE MANAGEMENT*.

Colella JP, Lan T, Talbot SL, Lindqvist C, Cook JA. 2021. Whole-genome Resequencing Reveals Persistence of Forest-Associated Mammals in Late Pleistocene Refugia along North America's North Pacific Coast. *J. Biogeogr.* 48:1153–1169.

Combe FJ, Jaster L, Ricketts A, Haukos D, Hope AG. 2021. Population Genomics of Free-ranging Great Plains White-tailed and Mule deer Reflects a Long History of Inter-specific Hybridization. *Evolutionary Applications* 15:111–132.

Commerford JL, Gittens G, Gainforth S, Wilson JJ, Bird BW. 2022. Differences in forest composition following two periods of settlement by pre-Columbian Native Americans. *Veget Hist Archaeobot* 31:467–480.

Cronin MA. 1991. Mitochondrial and Nuclear Genetic Relationships of Deer (Odocoileus spp.) in Western North America. *Can. J. Zool.* 69:1270–1279.

Danecek P, Auton A, Abecasis G, Albers CA, Banks E, DePristo MA, Handsaker RE, Lunter G, Marth GT, Sherry ST, et al. 2011. The variant call format and VCFtools. *Bioinformatics* 27:2156–2158.

Dawe KL, Boutin S. 2016. Climate change is the primary driver of white-tailed deer (Odocoileus virginianus) range expansion at the northern extent of its range; land use is secondary. *Ecol Evol* 6:6435–6451.

Dedato MN, Robert C, Taillon J, Shafer ABA, Côté SD. 2022. Demographic history and conservation genomics of caribou (Rangifer tarandus) in Québec. *Evolutionary Applications* 15:2043–2053.

Deer Friendly. Deer Population. *Deer Friendly* [Internet]. Available from: https://www.deerfriendly.com/decline-of-deer-populations

Derr JN. 1991. Genetic Interactions between White-Tailed and Mule Deer in the Southwestern United States. *The Journal of Wildlife Management* 55:228.

DeVivo MT, Edmunds DR, Kauffman MJ, Schumaker BA, Binfet J, Kreeger TJ, Richards BJ, Schätzl HM, Cornish TE. 2017. Endemic chronic wasting disease causes mule deer population decline in Wyoming.Zabel MD, editor. *PLoS ONE* 12:e0186512.

Deyoung RW, Demarais S, Honeycutt RL, Rooney AP, Gonzales RA, Gee KL. 2003. Genetic Consequences of White-tailed Deer (Odocoileus virginianus) Restoration in Mississippi. *Molecular Ecology* 12:3237–3252.

Dormann CF, Elith J, Bacher S, Buchmann C, Carl G, Carré G, Marquéz JRG, Gruber B, Lafourcade B, Leitão PJ, et al. 2013. Collinearity: a review of methods to deal with it and a simulation study evaluating their performance. *Ecography* 36:27–46.

Dussex N, Alberti F, Heino MT, Olsen R-A, van der Valk T, Ryman N, Laikre L, Ahlgren H, Askeyev IV, Askeyev OV, et al. 2020. Moose Genomes Reveal Past Glacial Demography and the Origin of Modern Lineages. *BMC Genomics* 21:854.

Ellsworth DL, Honeycutt RL, Silvy NJ, Bickham JW, Klimstra WD. 1994. Historical Biogeography and Contemporary Patterns Of Mitochondrial DNA Variation In White-Tailed Deer From The Southeastern United States. *Evolution* 48:122–136.

Ersmark E, Baryshnikov G, Higham T, Argant A, Castaños P, Döppes D, Gasparik M, Germonpré M, Lidén K, Lipecki G, et al. 2019. Genetic turnovers and northern survival during the last glacial maximum in European brown bears. *Ecol Evol* 9:5891–5905.

Evanno G, Regnaut S, Goudet J. 2005. Detecting the Number of Clusters of Individuals Using the Software Structure: a Simulation Study. *Mol Ecol* 14:2611–2620.

Ewels P, Magnusson M, Lundin S, Käller M. 2016. MultiQC: Summarize Analysis Results for Multiple Tools and Samples in a Single Report. *Bioinformatics* 32:3047–3048.

Ferchaud A-L, Perrier C, April J, Hernandez C, Dionne M, Bernatchez L. 2016. Making sense of the relationships between Ne, Nb and Nc towards defining conservation thresholds in Atlantic salmon (Salmo salar). *Heredity* 117:268–278.

Fick SE, Hijmans RJ. 2017. WorldClim 2: new 1-km spatial resolution climate surfaces for global land areas. *International Journal of Climatology* 37:4302–4315.

Forrester TD, Wittmer HU. 2013. A review of the population dynamics of mule deer and black-tailed deer Odocoileus hemionus in North America: Population dynamics of mule deer and black-tailed deer. *Mammal Review* 43:292–308.

Frankham R. 1995. Effective population size/adult population size ratios in wildlife: a review. *Genet. Res.* 66:95–107.

Frankham R. 2005. Genetics and extinction. *Biological Conservation* 126:131–140.

Fulton AE, Yansa CH. 2021. Onset of the Paleoanthropocene in the Lower Great Lakes Region of North America: An Archaeological and Paleoecological Synthesis. *Annals of the American Association of Geographers* 111:771–783.

Gajewski K, Kriesche B, Chaput MA, Kulik R, Schmidt V. 2019. Human–vegetation interactions during the Holocene in North America. *Veget Hist Archaeobot* 28:635–647.

Garrison E, Kronenberg ZN, Dawson ET, Pedersen BS, Prins P. 2022. A spectrum of free software tools for processing the VCF variant call format: vcflib, bio-vcf, cyvcf2, hts-nim and slivar.Schneidman-Duhovny D, editor. *PLoS Comput Biol* 18:e1009123.

Gill RB. 1999. Declining Mule Deer Populations in Colorado: Reasons and Responses (a report to the Colorado Legislature, November 1999). 58: Colorado Division of Wildlife

Gowan EJ, Zhang X, Khosravi S, Rovere A, Stocchi P, Hughes ALC, Gyllencreutz R, Mangerud J, Svendsen J-I, Lohmann G. 2021. A new global ice sheet reconstruction for the past 80 000 years. *Nat Commun* 12:1199.

Greenslade AD. 1998. Inter- and intraspecific phylogeography of North American Odocoileus Deer based on mitochondrial DNA sequences. Available from: https://research.library.mun.ca/1190/

Grinberg S. 2019. findPeaks. *GitHub* [Internet]. Available from: https://github.com/stas-g/findPeaks/blob/master/find_peaks.R

Grossen C, Guillaume F, Keller LF, Croll D. 2020. Purging of highly deleterious mutations through severe bottlenecks in Alpine ibex. *Nat Commun* 11:1001.

Gruell GE. 1986. Post-1900 mule deer irruptions in the Intermountain West: Principal cause and influences. Ogden, UT: U.S. Department of Agriculture, Forest Service, Intermountain Research Station Available from: https://www.fs.usda.gov/treesearch/pubs/37804

Gutenkunst RN, Hernandez RD, Williamson SH, Bustamante CD. 2009. Inferring the Joint Demographic History of Multiple Populations from Multidimensional SNP Frequency Data.McVean G, editor. *PLoS Genet* 5:e1000695.

Hahn MW. 2018. Molecular population genetics. New York : Sunderland, MA: Oxford University Press ; Sinauer Associates

Heffelfinger J, Krausman PR eds. 2023. Ecology and management of black-tailed and mule deer of North America. First edition. Boca Raton, FL: CRC Press

Hempel E, Bibi F, Faith JT, Koepfli K-P, Klittich AM, Duchêne DA, Brink JS, Kalthoff DC, Dalén L, Hofreiter M, et al. 2022. Blue Turns to Gray: Paleogenomic Insights into the Evolutionary History and Extinction of the Blue Antelope (Hippotragus leucophaeus).Lu J, editor. *Molecular Biology and Evolution* 39:msac241.

Hewitt DG. 2011. Biology and management of white-tailed deer. Boca Raton: CRC Press Available from: http://site.ebrary.com/id/11007093

Hijmans RJ. 2022. raster: Geographic Data Analysis and Modeling. Available from: https://CRAN.R-project.org/package=raster

IPCC. 2022. Climate change 2022: Impacts, adaptation and vulnerability. :3–33.

Ito T, Hayakawa T, Suzuki–Hashido N, Hamada Y, Kurihara Y, Hanya G, Kaneko A, Natsume T, Aisu S, Honda T, et al. 2021. Phylogeographic History of Japanese Macaques. *J Biogeogr*:jbi.14087.

Jensen WF, Bleich VC, Whittaker DG. 2023. Historical Trends in Black-tailed Deer, Mule Deer, and Their Habitats. In: Heffelfinger J, Krausman PR, Cox A, editors. Ecology and management of black-tailed and mule deer of North America. First edition. Boca Raton, FL: CRC Press.

Kessler C, Wootton E, Shafer ABA. 2023. Speciation without gene-flow in hybridizing deer. *Molecular Ecology* 32:1117–1132.

Kopelman NM, Mayzel J, Jakobsson M, Rosenberg NA, Mayrose I. 2015. Clumpak: a Program for Identifying Clustering Modes and Packaging Population Structure Inferences Across K. *Mol Ecol Resour* 15:1179–1191.

Korneliussen TS, Albrechtsen A, Nielsen R. 2014. ANGSD: Analysis of Next Generation Sequencing Data. *BMC Bioinformatics* 15:356.

Kvalnes T, Saether B-E, Haanes H, Røed KH, Engen S, Solberg EJ. 2016. Harvest-induced phenotypic selection in an island population of moose, Alces alces. *Evolution* 70:1486–1500.

Lamb S, Taylor AM, Hughes TA, McMillan BR, Larsen RT, Khan R, Weisz D, Dudchenko O, Aiden EL, Edelman NB, et al. 2021. De novo chromosome-length assembly of the mule deer (Odocoileus hemionus) genome. *Gigabyte* 2021:1–13.

Latch EK, Heffelfinger JR, Fike JA, RHODES Jr OE. 2009. Species-wide Phylogeography of North American Mule Deer (Odocoileus hemionus): Cryptic Glacial Refugia and Postglacial Recolonization. *Molecular Ecology* 18:1730–1745.

Latch EK, Reding DM, Heffelfinger JR, Alcalá-Galván CH, Rhodes OE. 2014. Range-wide Analysis of Genetic Structure in a Widespread, Highly Mobile Species (Odocoileus hemionus) Reveals the Importance of Historical Biogeography. *Mol Ecol* 23:3171–3190.

Li H, Durbin R. 2009. Fast and Accurate Short Read Alignment with Burrows-Wheeler Transform. *Bioinformatics* 25:1754–1760.

Li H, Durbin R. 2011. Inference of human population history from individual whole-genome sequences. *Nature* 475:493–496.

Li H, Handsaker B, Wysoker A, Fennell T, Ruan J, Homer N, Marth G, Abecasis G, Durbin R, 1000 Genome Project Data Processing Subgroup. 2009. The Sequence Alignment/Map format and SAMtools. *Bioinformatics* 25:2078–2079.

Lindo J, Huerta-Sánchez E, Nakagome S, Rasmussen M, Petzelt B, Mitchell J, Cybulski JS, Willerslev E, DeGiorgio M, Malhi RS. 2016. A time transect of exomes from a Native American population before and after European contact. *Nat Commun* 7:13175.

Loog L, Thalmann O, Sinding MS, Schuenemann VJ, Perri A, Germonpré M, Bocherens H, Witt KE, Samaniego Castruita JA, Velasco MS, et al. 2020. Ancient DNA suggests modern wolves trace their origin to a Late Pleistocene expansion from Beringia. *Mol Ecol* 29:1596–1610.

Lorenzen ED, Nogués-Bravo D, Orlando L, Weinstock J, Binladen J, Marske KA, Ugan A, Borregaard MK, Gilbert MTP, Nielsen R, et al. 2011. Species-specific responses of Late Quaternary megafauna to climate and humans. *Nature* 479:359–364.

Lynch VJ, Bedoya-Reina OC, Ratan A, Sulak M, Drautz-Moses DI, Perry GH, Miller W, Schuster SC. 2015. Elephantid Genomes Reveal the Molecular Bases of Woolly Mammoth Adaptations to the Arctic. *Cell Reports* 12:217–228.

Martchenko D, Shafer ABA. 2023. Contrasting whole-genome and reduced representation sequencing for population demographic and adaptive inference: an alpine mammal case study. *Heredity* [Internet]. Available from: https://www.nature.com/articles/s41437-023-00643-4

Martin M, Patterson M, Garg S, O Fischer S, Pisanti N, Klau GW, Schöenhuth A, Marschall T. 2016. WhatsHap: Fast and Accurate Read-based Phasing. Bioinformatics Available from: http://biorxiv.org/lookup/doi/10.1101/085050

Martin S. 2021. genomics_general. *GitHub* [Internet]. Available from: https://github.com/simonhmartin/genomics_general

Mautz W, Pekins P, Warren J. 1985. Cold temperature effects on metabolic rate of white-tailed, mule, and black-tailed deer in winter coat. *Biology of deer production. Bulletin* 22:453–457.

McDonald JS, Miller KV, Association QDM, Resources DBWS of F. 2004. A History of White-tailed Deer Restocking in the United States, 1878 to 2004. Quality Deer Management Assoc. Available from: https://books.google.ca/books?id=fv_oGwAACAAJ

McKenna A, Hanna M, Banks E, Sivachenko A, Cibulskis K, Kernytsky A, Garimella K, Altshuler D, Gabriel S, Daly M, et al. 2010. The Genome Analysis Toolkit: A MapReduce framework for analyzing next-generation DNA sequencing data. *Genome Research* 20:1297–1303.

Meiri M, Lister A, Kosintsev P, Zazula G, Barnes I. 2020. Population dynamics and range shifts of moose (Alces alces) during the Late Quaternary. *J Biogeogr* 47:2223–2234.

Meisner J, Albrechtsen A. 2018. Inferring Population Structure and Admixture Proportions in Low-Depth NGS Data. *Genetics* 210:719–731.

Meltzer DJ. 2020. Overkill, glacial history, and the extinction of North America's Ice Age megafauna. *Proc. Natl. Acad. Sci. U.S.A.* 117:28555–28563.

Moscarella RA, Aguilera M, Escalante AA. 2003. Phylogeography, Population Structure, and Implications for Conservation of White-tailed Deer (Odocoileus Virginianus) in Venezuela. *Journal of Mammalogy* 84:1300–1315.

O'Connell J, Gurdasani D, Delaneau O, Pirastu N, Ulivi S, Cocca M, Traglia M, Huang J, Huffman JE, Rudan I, et al. 2014. A General Approach for Haplotype Phasing across the Full Spectrum of Relatedness.Gibson G, editor. *PLoS Genet* 10:e1004234.

Oksanen J, Simpson GL, Blanchet FG, Kindt R, Legendre P, Minchin PR, O'Hara RB, Solymos P, Stevens MHH, Szoecs E, et al. 2022. vegan: Community Ecology Package. Available from: https://CRAN.R-project.org/package=vegan

Palkopoulou E, Mallick S, Skoglund P, Enk J, Rohland N, Li H, Omrak A, Vartanyan S, Poinar H, Götherström A, et al. 2015. Complete Genomes Reveal Signatures of Demographic and Genetic Declines in the Woolly Mammoth. *Current Biology* 25:1395–1400.

Palstra FP, Ruzzante DE. 2008. Genetic estimates of contemporary effective population size: what can they tell us about the importance of genetic stochasticity for wild population persistence? *Molecular Ecology* 17:3428–3447.

Pamilo P, Savolainen O. 2004. Post-Glacial Colonization, Drift, Local Selection and Conservation Value of Populations: A Northern Perspective. *Hereditas* 130:229–238.

Peart CR, Tusso S, Pophaly SD, Botero-Castro F, Wu C-C, Aurioles-Gamboa D, Baird AB, Bickham JW, Forcada J, Galimberti F, et al. 2020. Determinants of genetic variation across eco-evolutionary scales in pinnipeds. *Nat Ecol Evol* 4:1095–1104.

Pedersen BS, Quinlan AR. 2018. Mosdepth: Quick Coverage Calculation for Genomes and Exomes.Hancock J, editor. *Bioinformatics* 34:867–868.

Peres TM, Altman H. 2018. The Magic of Improbable Appendages: Deer Antler Objects in the Archaeological Record of the American South. *Journal of Archaeological Science: Reports* 20:888–895.

Portik DM, Leaché AD, Rivera D, Barej MF, Burger M, Hirschfeld M, Rödel M, Blackburn DC, Fujita MK. 2017. Evaluating mechanisms of diversification in a Guineo-Congolian tropical forest frog using demographic model selection. *Mol Ecol* 26:5245–5263.

Pundir S, Martin MJ, O'Donovan C, The UniProt Consortium. 2016. UniProt Tools. *Current Protocols in Bioinformatics* [Internet] 53. Available from: https://onlinelibrary.wiley.com/doi/10.1002/0471250953.bi0129s53

R Core Team. 2021. R: A Language and Environment for Statistical Computing. Vienna, Austria: R Foundation for Statistical Computing Available from: https://www.R-project.org/

Roycroft E, MacDonald AJ, Moritz C, Moussalli A, Portela Miguez R, Rowe KC. 2021. Museum genomics reveals the rapid decline and extinction of Australian rodents since European settlement. *Proc Natl Acad Sci USA* 118:e2021390118.

Russell T, Cullingham C, Ball M, Pybus M, Coltman D. 2021. Extent and direction of introgressive hybridization of mule and white-tailed deer in western Canada. *Evol Appl* 14:1914–1925.

Santiago E, Novo I, Pardiñas AF, Saura M, Wang J, Caballero A. 2020. Recent Demographic History Inferred by High-Resolution Analysis of Linkage Disequilibrium.Kim Y, editor. *Molecular Biology and Evolution* 37:3642–3653.

Schiffels S, Durbin R. 2014. Inferring Human Population Size and Separation History from Multiple Genome Sequences. *Nat Genet* 46:919–925.

Schiffels S, Wang K. 2020. MSMC and MSMC2: The Multiple Sequentially Markovian Coalescent. In: Dutheil JY, editor. Statistical Population Genomics. Vol. 2090. Methods in Molecular Biology. New York, NY: Springer US. p. 147–166. Available from: https://link.springer.com/10.1007/978-1-0716-0199-0_7

Seabury CM, Oldeschulte DL, Bhattarai EK, Legare D, Ferro PJ, Metz RP, Johnson CD, Lockwood MA, Nichols TA. 2020. Accurate Genomic Predictions for Chronic Wasting Disease in U.S. White-Tailed Deer. *G3 Genes|Genomes|Genetics* 10:1433–1441.

Shafer ABA, Cullingham CI, Côté SD, Coltman DW. 2010. Of Glaciers and Refugia: a Decade of Study Sheds New Light on the Phylogeography of Northwestern North America. *Molecular Ecology* 19:4589–4621.

Shafer ABA, Gattepaille LM, Stewart REA, Wolf JBW. 2015. Demographic inferences using short-read genomic data in an approximate Bayesian computation framework: in silico evaluation of power, biases and proof of concept in Atlantic walrus. *Mol Ecol* 24:328–345.

Skotte L, Korneliussen TS, Albrechtsen A. 2013. Estimating Individual Admixture Proportions from Next Generation Sequencing Data. *Genetics* 195:693–702.

Smith BT, Gehara M, Harvey MG. 2021. The demography of extinction in eastern North American birds. *Proc. R. Soc. B.* 288:20201945.

Stevens N, Bond W, Feurdean A, Lehmann CER. 2022. Grassy Ecosystems in the Anthropocene. *Annu. Rev. Environ. Resour.* 47:261–289.

Stewart M, Carleton WC, Groucutt HS. 2021. Climate change, not human population growth, correlates with Late Quaternary megafauna declines in North America. *Nat Commun* 12:965.

Stuart AJ. 2015. Late Quaternary megafaunal extinctions on the continents: a short review: LATE QUATERNARY MEGAFAUNAL EXTINCTIONS. *Geol. J.* 50:338–363.

Szpiech ZA. 2021. selscan 2.0: scanning for sweeps in unphased data. Evolutionary Biology Available from: http://biorxiv.org/lookup/doi/10.1101/2021.10.22.465497

Tarasov A, Vilella AJ, Cuppen E, Nijman IJ, Prins P. 2015. Sambamba: fast processing of NGS alignment formats. *Bioinformatics* 31:2032–2034.

Tavares GM, Reales G, Bortolini MC, Fagundes NJR. 2019. Measuring the impact of European colonization on Native American populations in Southern Brazil and Uruguay: Evidence from mtDNA. *Am J Hum Biol* 31:e23243.

U.S. Fish & Wildlife Service. 1967. Endangered Species List.

Van De Walle J, Pigeon G, Zedrosser A, Swenson JE, Pelletier F. 2018. Hunting regulation favors slow life histories in a large carnivore. *Nat Commun* 9:1100.

Villanova VL, Hughes PT, Hoffman EA. 2017. Combining genetic structure and demographic analyses to estimate persistence in endangered Key deer (Odocoileus virginianus clavium). *Conserv Genet* 18:1061–1076.

Wang K, Mathieson I, O'Connell J, Schiffels S. 2020. Tracking Human Population Structure through Time from Whole Genome Sequences.Schierup MH, editor. *PLoS Genet* 16:e1008552.

Waples RS, Luikart G, Faulkner JR, Tallmon DA. 2013. Simple life-history traits explain key effective population size ratios across diverse taxa. *Proc. R. Soc. B.* 280:20131339.

Webb GK. 2018. Searching the internet to estimate deer population trends in the U.S., California, and Connecticut. *IIS* 19:163–173.

Weitzel EM. 2021. Investigating overhunting of white-tailed deer (Odocoileus virginianus) in the late Holocene Middle Tennessee River Valley. *Southeastern Archaeology* 40:1–19.

Wilder AP, Supple MA, Subramanian A, Mudide A, Swofford R, Serres-Armero A, Steiner C, Koepfli K-P, Genereux DP, Karlsson EK, et al. 2023. The contribution of historical processes to contemporary extinction risk in placental mammals. *Science* 380:eabn5856.

Willerslev E, Meltzer DJ. 2021. Peopling of the Americas as inferred from ancient genomics. *Nature* 594:356–364.

Woinarski JCZ, Burbidge AA, Harrison PL. 2015. Ongoing unraveling of a continental fauna: Decline and extinction of Australian mammals since European settlement. *Proc. Natl. Acad. Sci. U.S.A.* 112:4531–4540.

Wolverton S, Nagaoka L, Densmore J, Fullerton B. 2008. White-tailed deer harvest pressure & within-bone nutrient exploitation during the mid- to late Holocene in southeast Texas. *Before Farming* 2008:1–23.

Wootton E, Robert C, Taillon J, Côté SD, Shafer ABA. 2023. Genomic health is dependent on long-term population demographic history. *Molecular Ecology* 32:1943–1954.

Wright EA, Roberts EK, Platt RN, Bayouth JV, Conway WC, Bradley RD. 2022. Mitochondrial capture and subsequent genetic divergence generates a novel haplogroup: evidence from ancient and ongoing hybridization in mule and white-tailed deer. *Journal of Mammalogy* 103:723–736.

Zamorano LS, Gompert Z, Fronhofer EA, Feder JL, Nosil P. 2023. A stabilizing eco-evolutionary feedback loop in the wild. *Current Biology* 33:3272-3278.e3.

Tables

Table 1: Tajima's D, nucleotide diversity and F_{ROH} for our four populations, F_{ROH} as percentage of the N90 scaffolds.

	Tajima's D	**Nucleotide diversity (π)**	**F_{ROH}**
WTD_{ML}	-0.89	0.0068	0.89 %
WTD_{KEY}	0.11	0.0038	1.38 %
MD_{MD}	-0.29	0.0036	0.30 %
MD_{BTD}	-0.13	0.0037	0.28 %

Table 2: Best model parameter values from δaδi per comparison and corresponding 95% CI computed on 100 bootstraps. Output values converted by solving for $\Theta = 4N_{ref}\mu L$.

		nu				**m**			**T**				
	Theta	**nu1**	**nu2**	**nu3**	**nuA**	**m1**	**m2**	**mA**	**T1**	**T1a**	**T1b**	**T2**	**T3**
WTD_{KEY} & WTD_{ML} & MD													
Parameters	21'150	0.56	1.73	0.20	4.02	0.86	2.15	-	0.57	-	-	0.12	0.02
2.5% CI		0.44	1.34	0.18	0.06	0.07	0.11	-	0.03	-	-	0.02	0.06
97.5% CI		2.61	7.47	2.04	24.23	0.49	2.70	-	3.27	-	-	3.95	4.10
Converted parameters		51'265	158'495	17'890	368'035	$4.7e^{-6}$	$1.2e^{-5}$	-	209'083	-	-	43'902	6'219
WTD_{ML} & MD_{BTD} & MD_{MD}													
Parameters	20'887	2.09	0.29	0.27	0.84	0.79	0.79	0.02	-	0.11	0.86	0.04	-
2.5% CI		1.17	0.13	0.10	0.07	0.04	0.10	0.03	-	0.04	0.05	0.02	-
97.5% CI		10.03	5.15	9.23	12.95	0.62	12.91	17.37	-	5.07	14.09	8.98	-
Converted parameters		188'752	26'276	23'990	75'439	$4.4e^{-6}$	$4.4e^{-6}$	$1.0e^{-7}$	-	41'080	309'923	12'826	-

Table 3: Anova of the RDA for full and conditional models as well as number of outlier SNPs for each predictor in the full model. Significant p-values are highlighted in bold.

		Adjusted R^2	*bio1*	*bio2*	*bio8*	*bio12*	*bio14*	*bio15*	*bio16*	*bio18*	*Longitude*	*Species*
Interspecies												
~ BIOs + Long + SP	P-value	16.55%	0.004	0.001	0.012	0.009	-	0.001	-	-	0.001	0.001
	Variance explained		2.58%	3.12%	1.95%	1.95%	-	3.54%	-	-	3.55%	7.96%
	number of outlier SNPs		5448	768	760	2491		47			2820	2101
MD												
~ BIOs + Long	P-value	8.82%	0.093	0.001	-	-	0.116	0.355	0.012	0.374	0.219	-
	Variance explained		5.67%	9.82%	-	-	5.48%	4.82%	6.72%	4.83%	5.04%	-
	number of outlier SNPs		99	540	-	-	690	1	4452	0	1652	-
~ BIOs + Condition(Long)	P-value	4.11%	0.119	0.032	-	-	0.167	0.336	0.003	0.476	-	-
	Variance explained		5.96%	6.23%	-	-	5.84%	5.53%	7.29%	5.35%	-	-
~ Condition(BIOs) + Long	P-value	0.35%	-	-	-	-	-	-	-	-	0.445	-
	Variance explained		-	-	-	-	-	-	-	-	8.05%	-
WTD												
~ BIOs + Long	P-value	6.32%	0.001	0.001	0.034	-	-	0.001	-	-	0.001	-
	Variance explained		3.37%	3.89%	2.11%	-	-	2.99%	-	-	2.96%	-
	number of outlier SNPs		5625	4487	1025	-	-	209	-	-	777	-
~ BIOs + Condition(Long)	P-value	4.64%	0.001	0.001	0.038	-	-	0.001	-	-	-	-
	Variance explained		3.50%	3.57%	2.18%	-	-	2.94%	-	-	-	-
~ Condition(BIOs) + Long	P-value	1.26%	-	-	-	-	-	-	-	-	0.001	-
	Variance explained		-	-	-	-	-	-	-	-	3.38%	-

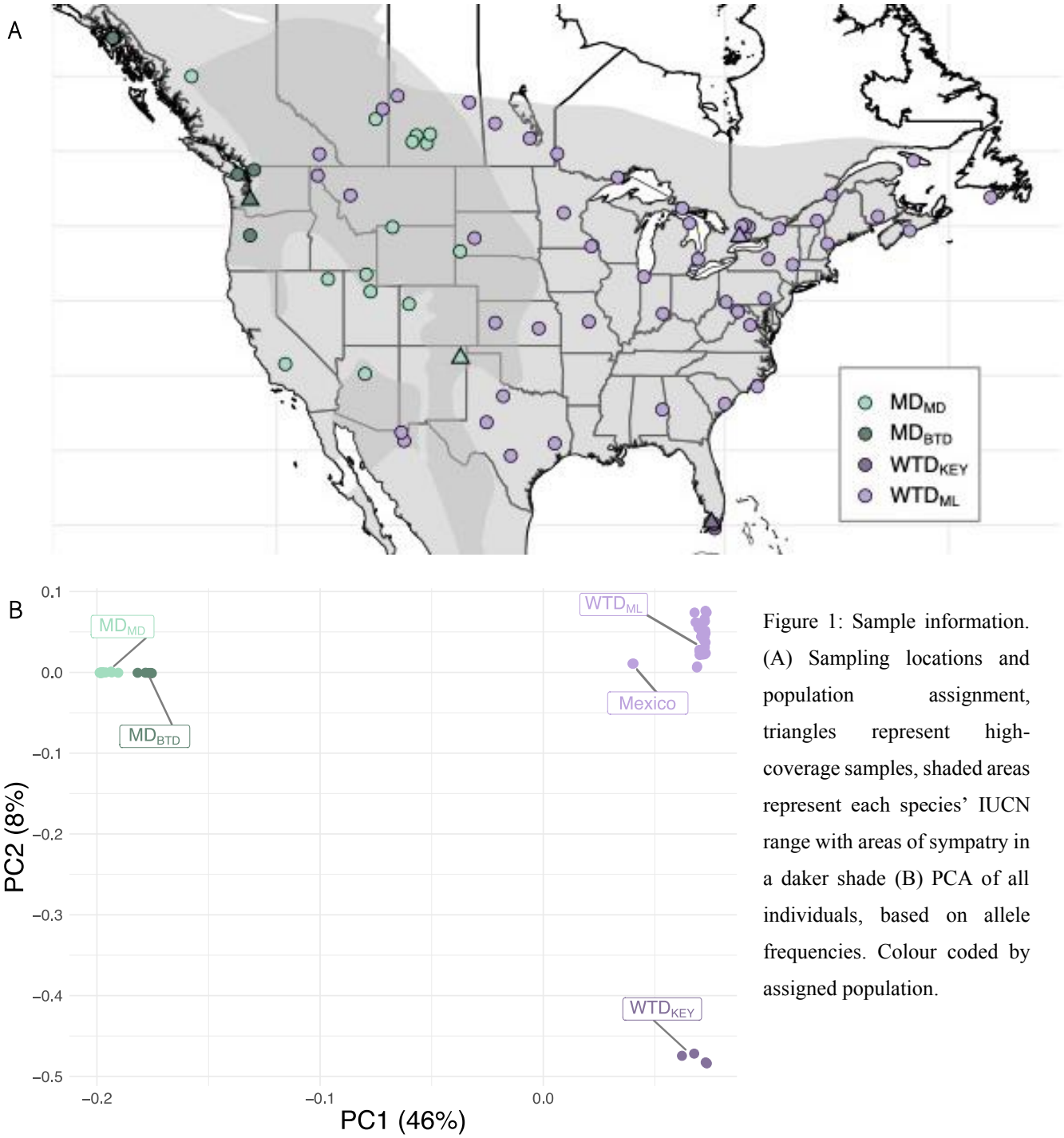

Figure 1: Sample information. (A) Sampling locations and population assignment, triangles represent high-coverage samples, shaded areas represent each species' IUCN range with areas of sympatry in a daker shade (B) PCA of all individuals, based on allele frequencies. Colour coded by assigned population.

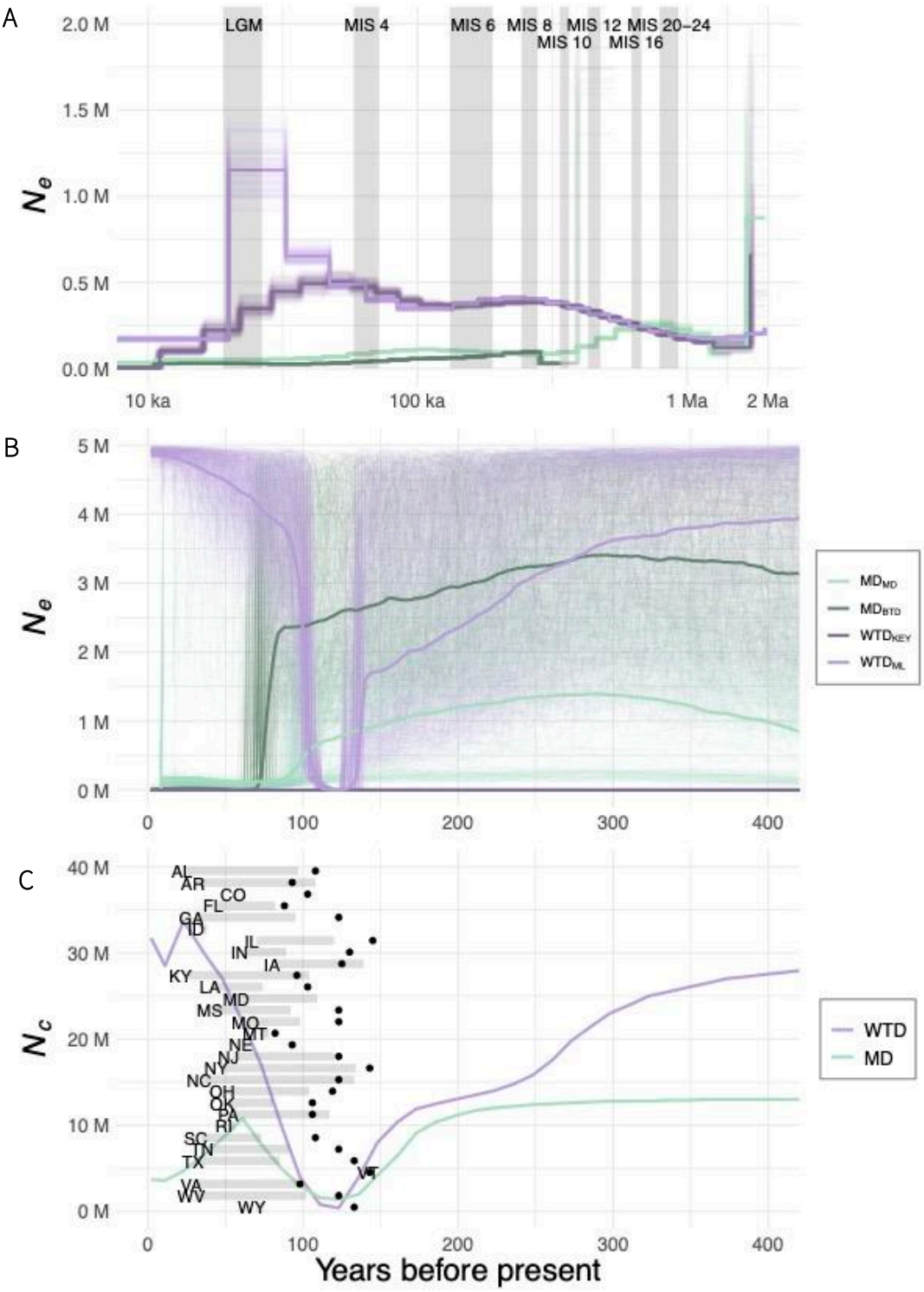

Figure 2: Demographic inference. (A) Changes in population size of four high coverage samples with bootstraps as estimated by MSMC2, shaded areas symbolise full glacial periods (Batchelor et al., 2019). (B) Recent changes in N_e computed by GONE on all samples with bootstraps. (C) Estimated WTD & MD population in the US from Webb (2018) with WTD restocking period for 30 US states (grey rectangles) and corresponding state's year with lowest WTD population (black points) from McDonald et al. (2004).

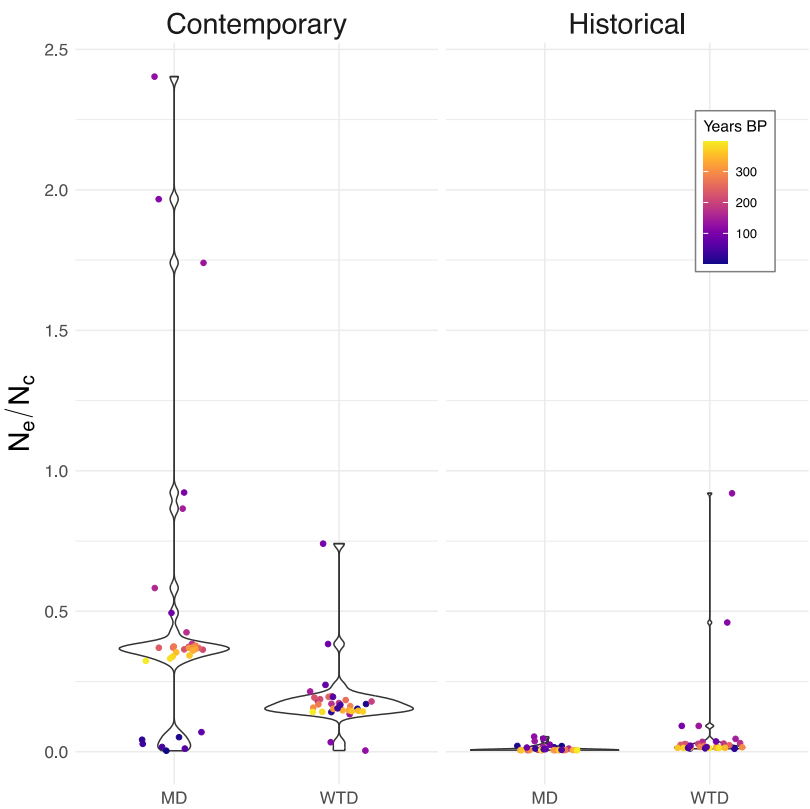

Figure 3: Contemporary and historical N_e/N_c ratio over time, point colour indicates time before present, N_e of the historical ratio taken from NuA values in the δaδi analysis.

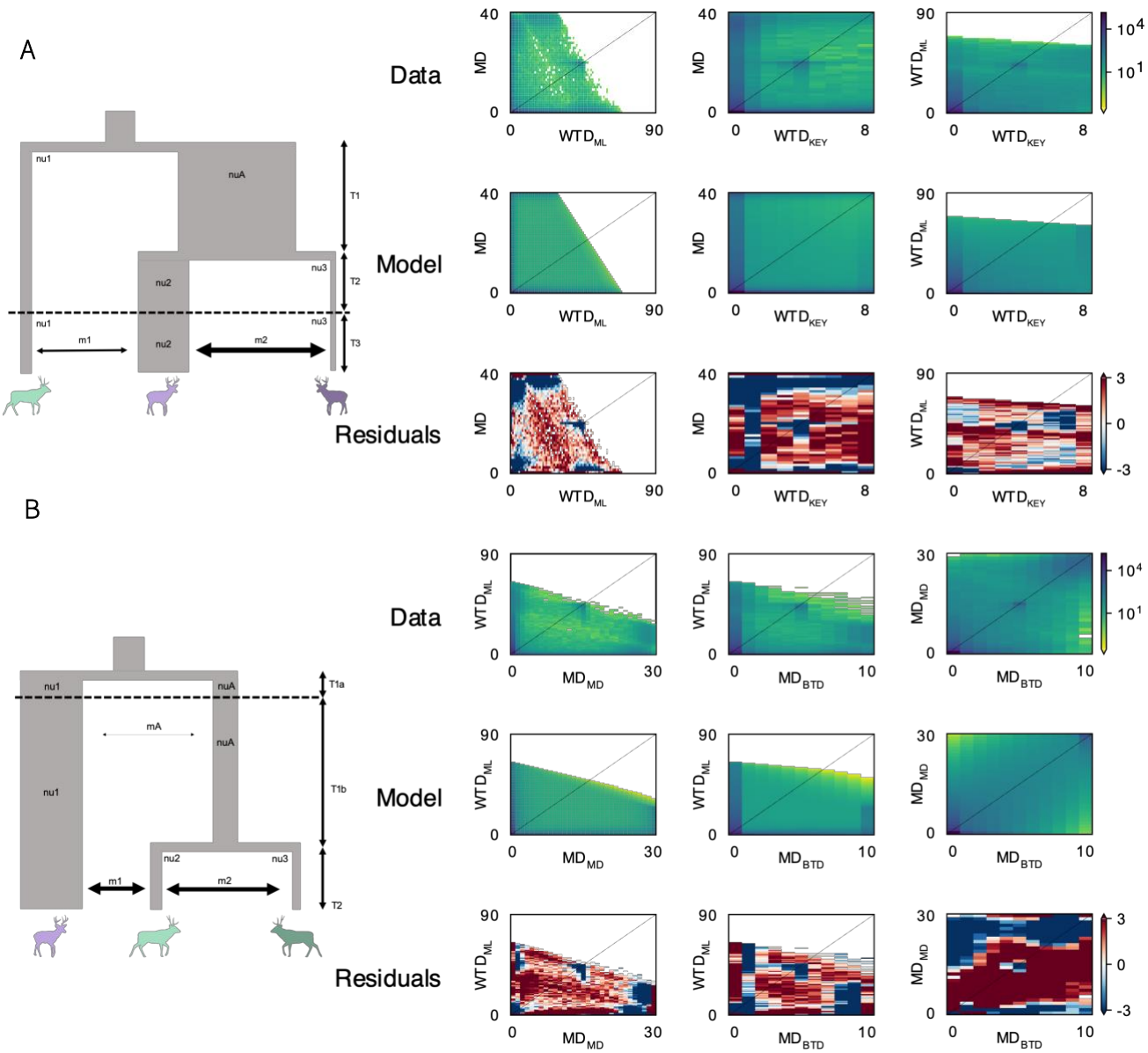

Figure 4: Three populations models in δaδI with best model schema on the left and 2D spectra on the right. (A) MD – WTD_{ML} – WTD_{KEY} comparisons, with MD in green, WTD_{ML} in light and WTD_{KEY} in dark purple. (B) WTD_{ML} – MD_{MD} – MD_{BTD} comparison with WTD_{ML} in light purple, MD_{MD} in light green and MD_{BTD} in dark green. Population sizes (nu) and migration rates (m) estimates to scale, time is not to scale.